In-structure shock assessment of underground structures with consideration of rigid body motion

Ma, Guowei; Zhou, Hongyuan; Chong, Karen

2011

Ma, G.W., Zhou, H. Y. & Chong, K. (2011). In-structure shock assessment of underground structures with consideration of rigid body motion. Journal of Engineering Mechanics, 137 (12), 797-806.

https://hdl.handle.net/10356/94969

https://doi.org/10.1061/(ASCE)EM.1943-7889.0000300

In-structure Shock Assessment of Underground Structures with Consideration of Rigid Body Motion

Guowei Ma[1]; Hongyuan Zhou[2]; and Karen Chong[3]

Abstract: The present study assesses the in-structure shock of an underground structure induced by a nearby subsurface detonation. Both the rigid body motion of the entirely buried structure and the local response of the structural element are considered in characterizing the in-structure shock. Soil-structure interaction, behaving as an interfacial damping, is taken into account and the effect of different surrounding soils is investigated. A response spectrum is plotted for assessing in-structure shock induced by a typical subsurface detonation and subsequently the safety of the internal facilities and equipments mounted on the buried structure is evaluated. For safety purpose, the protective structures are better constructed in a site with small acoustic impedance and large attenuation factor. Results show that the proposed in-structure shock assessment method is effective and can be used as a supplement to TM-5-855-1 and TM-5-1300.

CE Database subject headings: Underground structures; Blast loads; Soil-structure interactions; Structural response; Response spectra.

[1]Professor, School of Civil and Resource Engineering, Univ. of Western Australia, Crawley WA6009, Australia (corresponding author). E-mail: ma@civil.uwa.edu.au; and Associate Professor, School of Civil and Environmental Engineering, Nanyang Technological Univ., Singapore 639798, Singapore.
[2]Ph.D. Candidate, School of Civil and Environmental Engineering, Nanyang Technological Univ., Singapore 639798, Singapore.
[3]Research Manager, Defence Science and Technology Agency, Ministry of Defence, Singapore 109679, Singapore.

Introduction

Underground structures buried in soil usually provide safer shelters comparing to those aboveground due to the penetration resistance of the soil. However, in design of such underground buried structures, not only should the potential structural damage be assessed, but the shock load to the equipments contained in the structure should also be evaluated. The shock load from certain distance, normally with a very short duration such as some milliseconds, not causing significant damage to the structure, but vital to some delicate devices and equipments mounted internally on the structure, is termed as in-structure shock. In determination of the shock level within an underground structure, the most challenging task is to obtain the structural response to the shock in considering the soil-structure interaction (SSI). The effect of SSI can be neglected when the structure is subjected to an underground nuclear explosion since the overall motion, both that of the surrounding soil and that of the structure, can be assumed as the same as free field values because of the relative uniformity of the stress field. However, if the underground structure is under a shock caused by conventional weapons, the movement of the structure becomes more complex because the stress field is no longer uniform but attenuates with standoff distance quickly. In such cases, taking the SSI into account becomes a must.

To determine the structural shock response, various available numerical methods have been applied: the boundary element method (BEM) (Stamos and Beskos 1992), the finite-element method (FEM) (Yang 1997), the combined finite-difference method (FDM)/FEM (Steven and Krauthammer 1988; Chen and Krauthammer 1989), and the

combined smoothed particle hydrodynamics (SPH)/FEM (Wang et al. 2005; Lu 2005) have been applied. For the combined methods, the FDM or SPH was usually employed in the domain with large deformation, such as the soil near the detonation, wheareas the traditional FEM was adopted in the rest of the domain. In addition, the uncertainties in dynamic SSI were investigated numerically (Wong 1984). A distinct advantage of the numerical methods is that the comprehensive models can be established readily to represent the real detonation and response situations. However, the numerical methods could be very computationally intensive. In addition, relevant critical parameters are difficult to determine; further verification of the numerical models against analytical or experimental works is a prerequest.

Experimental results are considered to be most reliable and can be applied to verify analytical and numerical models. However, constructing and testing underground structures subjected to blast load is costly, labor-intensive, and time-consuming. In addition, because of the nature of such experiments, test results in open literatures is rare. In the research found, the rigid body motion (RBM) and SSI of an underground structure subjected to a subsurface explosion were studied through small scale experiment (Baylot and Hall 1995).

For theoretical methods, some design codes for evaluating the shock level of underground structures can be referred. Among the most frequently consulted are *Fundamentals of Protective Design for Conventional Weapons* (TM-5-855-1) (U.S. Army 1986) and *Structures to Resist the Effects of Accidental Explosion* (TM-5-1300) (U.S. Army 1990). According to TM-5-855-1, the in-structure displacement, velocity,

and acceleration are obtained by directly modifying the corresponding free-field values, which highly oversimplifies the problem. To effectively incorporate the SSI into the analysis, the structural response is taken into account to modify the loading applied on the structure (Wong and Weidlinger 1983). Further, the effects of structure motion on the soil flow near the structure and subsequent change in the structural loads and response were analyzed for a detonation very close to a structure (Baylot 2000). However, almost all the available analytical studies of underground structure dynamic response are based on single-degree-of-freedom (SDOF) models (Weidlinger and Hinman 1988; Alwis and Lam 1994; Chen and Chen 1996), which can be categorized into two approaches: 1) considering the entire structure as an rigid SDOF system, whereas the local response of the structural element is neglected; 2) simplifying a structural element as an SDOF system, whereas the global response of the structure was ignored. In fact, the SSI relies on the structural deformation;, therefore, a more appropriate consideration of the SSI requires adopting a continuous model.

When subjected to a subsurface detonation, in general, an underground structure undergoes two kinds of motions: RBM as a whole and local response of the structural element. To the writers' knowledge, a continuous model for underground structural response, induced by a subsurface explosion with consideration of RBM, has not been analytically established.

To assess the shock level within the underground structure more accurately, an analytical model consisting of the RBM and local deflection is presented in this study.

Due to the relative large distance between the detonation and the structure in which case no significant damage occurs, the effect of soil flow change on structural loads may be negligible (Baylot 2000). In the current model, the responses of the structural element are obtained in consideration of both the SSI and the RBM effects. The derived structural response then acts as the excitation for the equipments internally mounted on the structure. The response of the equipment thus can be obtained and compared with the specified tolerance to check its safety. The present paper mainly focuses on the derivation of the structural responses by combining the global RBM and the local element response, in which an interfacial damping is introduced to reflect the SSI.

Methodology

When subjected to a soil-transmitted blast load, the underground structure undergoes RBM as well as deflection simultaneously. It is difficult even impossible to obtain both the RBM and the deflection at the same time analytically. In the present study, to determine the gross response of certain structural element, the displacement of the structural element is decoupled into two parts: one from RBM and the other from the pure deflection. Based on this decoupling, the lower and upper bounds of the structural element are obtained. Consider two extreme cases:

(a) Without RBM, the load applied totally contributes to the deformation of the structural element.

(b) Without deflection, the load applied totally contributes to the RBM.

It is obvious that the response of case (a) is significantly greater than that of case (b) for a typical underground structure subjected to a subsurface detonation. Case study calculation results in the following section will confirm this.

In deriving the RBM response, the structure is assumed rigid and undergoes pure translation. Obviously, the assumption of rigid structure will lead to an over-prediction of the RBM response. Subsequently, the load allocated to cause pure deflection of the structural element is under-estimated.

The real situation is the soil-transmitted blast load contributes to both the RBM and the deflection simultaneously. The overly-predicted RBM and the under-estimated deformation will result in gross responses lower than the real situation. It is not conservative and can be considered as the lower bound of the gross response of the structural element.

Furthermore, the upper bound of the gross response is determined by assuming no RBM and the structural element only undergoes pure deflection.

With no doubt, the response of the structural element in real situation is in between of these upper and lower bounds. In a typical in-structure shock problem, the upper and lower bounds responses are close to each other thus the real response is approximately found. In the present study, the method is formulated analytically in detail and validated in a case study.

Shock load and soil-structure interaction

According to TM-5-855-1, the peak stress wave intensity induced by a subsurface

detonation of a conventional weapon is

$$P_0 = \beta f\left(\rho_s c_s\right)\left(\frac{R}{W^{1/3}}\right)^{-r} \tag{1}$$

where P_0 = peak free-field pressure; f = coupling factor of the explosion energy to soil; $\rho_s c_s$ = acoustic impedance of soil; r= attenuation factor of soil; W= TNT equivalent weight; R= distance measured from the explosion center to the structure; and β =160.

The shape of the shock wave depends on that of the charge. For a most frequently encountered point detonation, the shock wave develops and transmits to all directions spherically. In engineering practice, when the standoff distance is relatively large, the part of the wave encountering a structure is assumed to be an equivalent free field plane wave (U.S. Army 1986) as follows,

$$\sigma_f\left(t\right) = \begin{cases} P_0\alpha\left(1-\dfrac{t}{T_d}\right) & \text{for } t \le T_d \\ 0 & \text{for } t > T_d \end{cases} \tag{2a}$$

where α = reduction factor, defined as the ratio of the equivalent uniformly distributed load to the maximum pressure in the actual load distribution; and T_d = equivalent blast duration, equal to two times the arrival time of the shock wave from the detonation point to the structure (Weidlinger and Hinman 1988), such that

$$T_d = 2t_a \tag{2b}$$

According to Wong and Weidlinger (1983), the load applied on the underground structure is a free-field pressure overlapped with the interfacial pressure,

$$\sigma = \sigma_f + \sigma_i = 2\sigma_f - \rho c_s \dot{u} \tag{3}$$

where $\dot{u}$ = velocity of a certain material point in the structure. The above formula is valid only when the SSI exists, which implies that the soil has larger particle velocity

than the structure. If the soil particle velocity is smaller than that of the structure, the SSI vanishes and there is no load applied on the structural element from soil at this interface.

Rigid body motion of the entire structure

Conservatively, the most adverse situation is analyzed where the nearest point to the subsurface detonation is the center of certain structural element. If the underground explosion occurs in a location where the nearest point from the structure to the detonation is a corner, the problem is further complicated. In this situation, generally, the RBM of the assumed rigid structure will be a combination of translation and rotation, rather than pure translation, which is out of the scope of the current study.

For a box-type underground structure subjected to a blast load induced, generally, there are several loading phases for the RBM, loading only on the nearest structural element, loading on both nearest and farthest structural elements, loading only on the farthest element and the phase in which only the soil resistance exists on the farthest element. For a typical detonation case, the most important phase is the first one, in which the maximum acceleration and velocity of the entire structure always occur. Therefore only the first loading phase is considered (Weidlinger and Hinman 1988, 1991; Alwis and Lam 1994). As stated in the methodology, when analyzing the RBM, the structural deflection is ignored thus the structure is assumed as a rigid body. The friction between the side walls and the surrounding soil is negligible compared to the blast load thus it is ignored. In addition, among the resistances from the back side of

the structure, only the major part induced by the velocity difference between the structure and the surrounding soil is considered (Weidlinger and Hinman 1988, 1991; Alwis and Lam 1994).

Taking the SSI into consideration, we have:

$$M\frac{d^2U(t)}{dt^2}=A\left\{\left[\sigma_{f,\mathrm{N}}+\rho_s c_s\left(V_{\mathrm{N}}-\frac{dU(t)}{dt}\right)\right]-\rho_s c_s\frac{dU(t)}{dt}\right\} \tag{4}$$

where M = mass of the whole structure; A= area of a structural element subjected to a blast load; $\sigma_{f,\mathrm{N}}$ and V_{N}= free field pressure and soil particle velocity at the nearest structural element, respectively; and $U(t)$= RBM displacement of the structure. In consideration of $\sigma_{f,N}=\rho_s c_s V_{\mathrm{N}}$ and Eq. (2*a*), Eq. (4) becomes

$$\tau_0\frac{d^2U(t)}{dt^2}+\frac{dU(t)}{dt}=\frac{P_0\alpha}{\rho_s c_s}\left(1-\frac{t}{T_d}\right) \tag{5}$$

where $\tau_0=M/(2A\rho_s c_s)$ is defined as the characteristic response time.

With a stationary initial condition with zero displacement and zero velocity assumed for the structure, the time histories of the RBM which do not consider the structural deflection can be derived as:

$$U(t)=\frac{P_0\alpha}{\rho_s c_s}\left[\left(1+\frac{\tau_0}{T_d}\right)t-\frac{t^2}{2T_d}+\frac{\tau_0}{T_d}(\tau_0+T_d)\left(e^{-t/\tau_0}-1\right)\right] \tag{6a}$$

$$\dot{U}(t)=\frac{P_0\alpha}{\rho_s c_s}\left[\left(1+\frac{\tau_0}{T_d}\right)-\frac{t}{T_d}-\left(1+\frac{\tau_0}{T_d}\right)e^{-t/\tau_0}\right] \tag{6b}$$

$$\ddot{U}(t)=-\frac{P_0\alpha}{\rho_s c_s}\left[\frac{1}{T_d}-\left(\frac{1}{\tau_0}+\frac{1}{T_d}\right)e^{-t/\tau_0}\right] \tag{6c}$$

It is worth noting that the derived RBM response is obviously greater than that in the real situation by assuming no deflection, ignoring the side friction and some resistance from the back side.

Structural element response to shock load

Kirchhoff plate model

For a typical box-type underground structure, each of the structural elements is considered as a Kirchhoff plate in consideration that the thickness-to-span and the maximum-deflection-to-thickness ratios are, in any time, both smaller than 1/5, in which the Kirchhoff-Love plate theory can be applied. In a real structure, each plate of the buried structure is neither fixed nor simply supported to other structural elements. For safer consideration, the plate is assumed to be simply supported in the current analysis.

In the present study, in-structure shock rather than damage is of major concern. Therefore it is reasonable to assume that the structural response is within the elastic limit. According to Baylot and Hall (1995), in a small scale experiment, when the distance between the detonation and the structure is relatively large, the structure experiences a shock and the structural element deforms elastically without major damage. The governing equation for a plate subjected to dynamic load is:

$$D\nabla^4 w(x,y,t) + \rho h \frac{\partial^2 w(x,y,t)}{\partial t^2} = P(x,y,t) \tag{7}$$

In view of the SSI in Eq. (3), the governing equation can be rewritten as:

$$D\nabla^4 w(x,y,t) + \rho h \frac{\partial^2 w(x,y,t)}{\partial t^2} + \rho_s c_s \frac{\partial w(x,y,t)}{\partial t} = 2P_0 \alpha \left(1 - \frac{t}{T_d}\right) \tag{8}$$

where $D = Eh^3 / \left[12\left(1-\nu^2\right)\right]$ is the flexural rigidity of the plate; ρ and h= density

and thickness of the plate, respectively. Assume the displacement of the structural element as:

$$w(x,y,t) = U(t) + \sum_{m=1}^{\infty}\sum_{n=1}^{\infty} W_{mn}(x,y)\,\eta_{mn}(t) \tag{9}$$

recall that $U(t)$ = RBM displacement; $W_{mn}(x,y)$ = m, nth mode shape, in which m, n denote the order of the vibration in two orthogonal directions; and $\eta_{mn}(t)$ = generalized coordinate in the generalized space, or modal space. Since the RBM in fact is the zeroth order of the vibration mode and does not affect the deflection of the structural element, through analyzing the specific mode, with the simply supported boundary condition, the m, nth mode can be expressed as

$$W_{mn}(x,y) = \frac{2}{\sqrt{\rho hab}} \sin\frac{m\pi x}{a} \sin\frac{n\pi y}{b} \tag{10}$$

where a and b = in-plane dimensions of the plate, respectively.

Deformation Response in the blast duration

Substituting Eq. (9) into Eq. (8), and rewrite the governing equation:

$$\rho h\sum_{m=1}^{\infty}\sum_{n=1}^{\infty} W_{mn}(x,y)\,\ddot{\eta}_{mn}(t) + \rho_s c_s \sum_{m=1}^{\infty}\sum_{n=1}^{\infty} W_{mn}(x,y)\,\dot{\eta}_{mn}(t) +$$
$$D\sum_{m=1}^{\infty}\sum_{n=1}^{\infty} \pi^4 \left[\left(\frac{m}{a}\right)^2 + \left(\frac{n}{b}\right)^2\right]^2 W_{mn}(x,y)\,\eta_{mn}(t) = 2\sigma_f(t) - \rho h\ddot{U}(t) - \rho_s c_s \dot{U}(t) \tag{11}$$

According to the orthogonality condition of the normal modes, the governing equation for the m, nth mode is

$$\ddot{\eta}_{mn}(t) + \frac{\rho_s c_s}{\rho h}\dot{\eta}_{mn}(t) + \pi^4 \frac{D}{\rho h}\left[\left(\frac{m}{a}\right)^2 + \left(\frac{n}{b}\right)^2\right]^2 \eta_{mn}(t) = F_{mn}(t) \tag{12a}$$

$$F_{mn}(t)=\left[1-(-1)^m\right]\left[1-(-1)^n\right]\frac{2}{mn\pi^2}\sqrt{\frac{ab}{\rho h}}\left[2\sigma_f(t)-\rho h\ddot{U}(t)-\rho_s c_s\dot{U}(t)\right] \quad (12b)$$

To demonstrate the effect of the SSI, the *m*, *n*th interfacial damping ratio is defined as

$$\zeta_{mn}=\frac{\frac{\rho_s c_s}{\rho h}}{2\omega_{mn}}=\frac{\frac{\rho_s c_s}{\rho h}}{2\pi^2\sqrt{\frac{D}{\rho h}}\left[\left(\frac{m}{a}\right)^2+\left(\frac{n}{b}\right)^2\right]} \quad (13)$$

where ω_{mn} = *m*, *n*th natural frequency of the plate. The interfacial damping ratio, induced by the presence of the interface between the structure and the surrounding soil, delineates the SSI by incorporating nearly all the properties from both the structure and the soil, inclusive of the acoustic impedance of the soil, the in-plane dimensions, mode order numbers, density, thickness and flexural rigidity of the structural element. From the expression, one can know that the interfacial damping ratio decreases with the increase of orders in two directions, which means the damping ratios are greater for lower modes and smaller for higher modes. The same structure buried in different soils have different interfacial damping ratios. For a typical protective structure in certain kinds of soils, the first or first several modes of the structural element may be interfacially over-damped while the higher modes under-damped. The corresponding structural responses are derived as follows.

Case I: $\zeta_{mn}>1$

Assume the arrival time of the blast wave as the time origin. At zero time, both the displacement and the velocity are zero no matter in the physical space or the generalized space. Combining the governing equation and the initial conditions, for an interfacial damping ratio larger than 1, the local structural responses are obtained, e.g. the *m*, *n*th order contribution to the deflection is

$$w_{mn}\left(x,y,t\right)=\frac{2}{\sqrt{\rho hab}}\sin\frac{m\pi x}{a}\sin\frac{n\pi y}{b}\begin{Bmatrix}E_{mn}e^{D_{mn,3}t}+F_{mn}e^{D_{mn,4}t}\\+Q_{mn}\left[D_{mn,1}\left(D_{mn,5}-\omega_{mn}t\right)+\tau_0 D_{mn,2}e^{-t/\tau_0}\right]\end{Bmatrix} \quad (14)$$

where

$$E_{mn}=-\frac{Q_{mn}\left(\omega_{mn}D_{mn,1}+D_{mn,2}+D_{mn,1}D_{mn,4}D_{mn,5}+\tau_0 D_{mn,2}D_{mn,4}\right)}{D_{mn,4}-D_{mn,3}}$$

$$F_{mn}=\frac{Q_{mn}\left(\omega_{mn}D_{mn,1}+D_{mn,2}+D_{mn,1}D_{mn,3}D_{mn,5}+\tau_0 D_{mn,2}D_{mn,3}\right)}{D_{mn,4}-D_{mn,3}}$$

$$Q_{mn}=\left[1-\left(-1\right)^m\right]\left[1-\left(-1\right)^n\right]\frac{2}{mn\pi^2}\sqrt{\frac{ab}{\rho h}}$$

$$D_{mn,1}=\frac{P_0\alpha}{\omega_{mn}^3 T_d}$$

$$D_{mn,2}=\frac{\tau_0 P_0\alpha}{\omega_{mn}^2\tau_0^2-2\zeta_{mn}\omega_{mn}\tau_0+1}\left[\left(1+\frac{\tau_0}{T_d}\right)-\frac{1}{2\zeta_{mn}\omega_{mn}}\left(\frac{1}{\tau_0}+\frac{1}{T_d}\right)\right]$$

$$D_{mn,3}=\left(-\zeta_{mn}+\sqrt{\zeta_{mn}^2-1}\right)\omega_{mn}$$

$$D_{mn,4}=\left(-\zeta_{mn}-\sqrt{\zeta_{mn}^2-1}\right)\omega_{mn}$$

$$D_{mn,5}=\omega_{mn}\left(T_d-\tau_0\right)+\left(2\zeta_{mn}+\frac{1}{2\zeta_{mn}}\right)$$

the velocity contributed by *m*, *n*th mode is

$$\dot{w}_{mn}\left(x,y,t\right)=\frac{2}{\sqrt{\rho hab}}\sin\frac{m\pi x}{a}\sin\frac{n\pi y}{b}\begin{bmatrix}E_{mn}D_{mn,3}e^{D_{mn,3}t}+F_{mn}D_{mn,4}e^{D_{mn,4}t}\\-Q_{mn}\left(\omega_{mn}D_{mn,1}+D_{mn,2}e^{-t/\tau_0}\right)\end{bmatrix} \quad (15)$$

and the corresponding acceleration is

$$\ddot{w}_{mn}\left(x,y,t\right)=\frac{2}{\sqrt{\rho hab}}\sin\frac{m\pi x}{a}\sin\frac{n\pi y}{b}\left(E_{mn}D_{mn,3}^2e^{D_{mn,3}t}+F_{mn}D_{mn,4}^2e^{D_{mn,4}t}+\frac{Q_{mn}}{\tau_0}D_{mn,2}e^{-t/\tau_0}\right) \quad (16)$$

The aforementioned solutions are valid only in blast loading phase in which the

structural element deforms to the maximum deflection.

Case II: $\zeta_{mn} < 1$

When the interfacial damping ratio is smaller than 1, with the same method, the *m*, *n*th order contribution to the displacement is

$$w_{mn}(x,y,t) = \frac{2}{\sqrt{\rho hab}} \sin\frac{m\pi x}{a} \sin\frac{n\pi y}{b} \begin{Bmatrix} e^{-\zeta_{mn}\omega_{mn}t}\left[E_{mn}\sin D_{mn,6}t + F_{mn}\cos D_{mn,6}t\right] \\ +Q_{mn}\left[D_{mn,1}\left(D_{mn,5} - \omega_{mn}t\right) + \tau_0 D_{mn,2}e^{-t/\tau_0}\right] \end{Bmatrix} \quad (17)$$

where

$$E_{mn} = -\frac{Q_{mn}\left[\zeta_{mn}\omega_{mn}\left(D_{mn,1}D_{mn,5} + \tau_0 D_{mn,2}\right) - \omega_{mn}D_{mn,1} - D_{mn,2}\right]}{\sqrt{1-\zeta_{mn}^2}\,\omega_{mn}}$$

$$F_{mn} = -Q_{mn}\left(D_{mn,1}D_{mn,5} + \tau_0 D_{mn,2}\right)$$

$$D_{mn,6} = \sqrt{1-\zeta_{mn}^2}\,\omega_{mn}$$

$D_{mn,i}\,(i = 1, 2, 5)$ = same as defined in the previous section.

the velocity contribution of the *m*, *n*th mode is

$$\dot{w}_{mn}(x,y,t) = \frac{2}{\sqrt{\rho hab}} \sin\frac{m\pi x}{a} \sin\frac{n\pi y}{b} \begin{Bmatrix} -e^{-\zeta_{mn}\omega_{mn}t}\begin{bmatrix}\left(\zeta_{mn}\omega_{mn}E_{mn} + D_{mn,6}F_{mn}\right)\sin D_{mn,6}t \\ +\left(\zeta_{mn}\omega_{mn}F_{mn} - D_{mn,6}E_{mn}\right)\cos D_{mn,6}t\end{bmatrix} \\ -Q_{mn}\left(\omega_{mn}D_{mn,1} + D_{mn,2}e^{-t/\tau_0}\right) \end{Bmatrix} \quad (18)$$

and the corresponding acceleration is

$$\ddot{w}_{mn}(x,y,t) = \frac{2}{\sqrt{\rho hab}} \sin\frac{m\pi x}{a} \sin\frac{n\pi y}{b} \begin{Bmatrix} e^{-\zeta_{mn}\omega_{mn}t}\begin{bmatrix}\left(\zeta_{mn}^2\omega_{mn}^2E_{mn} + 2\zeta_{mn}\omega_{mn}D_{mn,6}F_{mn} - D_{mn,6}^2E_{mn}\right)\sin D_{mn,6}t \\ +\left(\zeta_{mn}^2\omega_{mn}^2F_{mn} - 2\zeta_{mn}\omega_{mn}D_{mn,6}E_{mn} - D_{mn,6}^2F_{mn}\right)\cos D_{mn,6}t\end{bmatrix} \\ +\frac{Q_{mn}}{\tau_0}D_{mn,2}e^{-t/\tau_0} \end{Bmatrix} \quad (19)$$

Again the results above are valid only in the time intersection of the blast duration and time period ranging from zero to maximum deflection.

In practical engineering, it stands very rare chance to have an interfacial damping ratio exactly equal to 1. However, if it happens, for mathematical derivation convenience and the physical nature, it can be considered as an interfacially over-damped case.

Gross response in the blast duration

The gross response of the structural element consisting of the RBM and pure deflection is of concern and is also the response lower bound when considering both the RBM and the deflection simultaneously. The response contribution by the pure deflection, under-estimated, is derived above.

When analyzing the RBM by assuming no deflection, the pure RBM responses are overly-predicted thus when analyzing the RBM and the deflection simultaneously, the force allocated for the RBM part $\rho h\ddot{U}(t)+\rho_s c_s\dot{U}(t)$ (see right hand side of the Eq. (11)) is also overly-predicted. Subsequently the RBM contribution to the gross response of the structural element is higher than that in the real situation.

Equations (20a)(20b) are the RBM velocity and acceleration time histories when considering RBM and deflection simultaneously.

$$\dot{U}_m(t)=\frac{P_0\alpha}{\rho_s c_s}\left\{e^{-\frac{t}{\tau_0}}\left[\left(\frac{2h}{h_e}-1\right)\left(\frac{1}{\tau_0}+\frac{1}{T_d}\right)t-1-\frac{2\tau_0}{T_d}\left(1-\frac{h}{h_e}\right)\right]+1-\frac{t}{T_d}+\frac{2\tau_0}{T_d}\left(1-\frac{h}{h_e}\right)\right\} \tag{20a}$$

$$\ddot{U}_m(t)=\frac{P_0\alpha}{\rho_s c_s}\left\{\frac{e^{-\frac{t}{\tau_0}}}{\tau_0}\left[-\left(\frac{2h}{h_e}-1\right)\left(\frac{1}{\tau_0}+\frac{1}{T_d}\right)t+\frac{2h}{h_e}+\frac{\tau_0}{T_d}\right]-\frac{1}{T_d}\right\} \tag{20b}$$

where $h_e = M/(\rho A)$ represents the effective thickness of the whole structure.

Equations (21a)(21b)(21c) are the pure deflection, gross velocity and gross acceleration time histories of the structural element while considering RBM and the deformation simultaneously:

$$w_d(x,y,t) = \sum_{m=1}^{\infty}\sum_{n=1}^{\infty} W_{mn}(x,y)\,\eta_{mn}(t) \tag{21a}$$

$$\dot{w}(x,y,t) = \dot{U}_m(t) + \sum_{m=1}^{\infty}\sum_{n=1}^{\infty} W_{mn}(x,y)\,\dot{\eta}_{mn}(t) \tag{21b}$$

$$\ddot{w}(x,y,t) = \ddot{U}_m(t) + \sum_{m=1}^{\infty}\sum_{n=1}^{\infty} W_{mn}(x,y)\,\ddot{\eta}_{mn}(t) \tag{21c}$$

Amongst, pure deflection, Eq. (21a), rather than the gross displacement, is of interest since only the pure deflection has contribution to the stress distribution in the structure element while the RBM displacement part has no contribution. For a typical in-structure shock problem, structural failure is not the major concern due to the thick wall and the relatively distant explosion location. The gross acceleration time history, Eq. (21c), consisting of the contributions both from the RBM and the pure deflection, is of most significance since it is the direct excitation for the inside device attached to the structural element and related to the force developed within the equipment and directly determine its safety.

The response after the blast duration can be calculated with the application of the terminal conditions of the blast duration phase as initial conditions. In fact, for a typical problem of in-structure shock of underground structure subjected to a subsurface detonation, the response time histories in the blast duration will suffice

since the acceleration response used to excite the device achieves peak value initially and decays at a high rate, making the major shock in the initial stage of the blast duration.

Theoretically, the exact responses are achieved by combining all the contributions of modes from first order to infinity. In fact, higher order modes generally make trivial contribution therefore finite modes are used to approximately represent the exact response. The number of modes needed depends on the physical nature of the problem (for dynamic problem with short load duration, more modes are needed) as well as the result accuracy desired. Generally, for a problem of an underground structure with typical geometrical configuration subjected to a typical subsurface-detonation induced blast, 20-30 modes in each direction is sufficient.

Until now, the lower bound responses of a structural element are derived. Further, the upper bound responses are calculated by assuming no RBM. Then the real responses can be approximately found.

A case study and discussions

Consider a box-shaped underground structure subjected to a subsurface detonation loading on one of its structural element, made of reinforced concrete with the Young's modulus of 30 GPa, the Poisson's ratio of 0.2, and the density of 2500 kg/m^3. The length, width, and height of the structure are assumed to be 12.8 m, 14 m, and 8 m, respectively. All the structural elements have the uniform thickness of 1 m. The surrounding soils are dry sand and two typical soils in Singapore, i.e. Kallang soil and

Bukit Timah soil (Anand 2007, properties are shown in Table 1), respectively. Amongst, Bukit Timah soil has the largest acoustic impedance and the smallest attenuation factor while the dry sand has the smallest acoustic impedance and the largest attenuation factor. The scaled distance, defined as the standoff distance divided by the cubic root of the TNT equivalent weight, is 2 m/kg$^{1/3}$ (R=10 m, W=125 kg). The shock load duration is 20 ms. All of the parameters used are typical for an underground detonation. First 30 modes in each direction are used to approximate the exact responses and the results converge without any "visible" oscillation.

Obviously, for a scenario that the detonation lies in the extended line through two opposite structural element centers, shown in Fig. 1, the center of the nearest plate to the detonation is the most dangerous point and needs special inspections.

Figure 2 gives the upper and lower bounds of structural element center pure deflection, gross velocity and gross acceleration surrounded by Kallang soil. The bounds of pure deflection of the element center are far from each other thus it is difficult to approximate the real deflection. As stated previously, deflection is not the major concern for in-structure shock problem due to the thick structure wall and relatively distant standoff. In this case, the maximum deflection is smaller than 14 mm, compared to the 1 m thickness, the deformation is elastic. Amongst, for acceleration time history, the two bounds are close and the real acceleration can be readily approximated.

In engineering practice, the relationship between the maximum response values and the scaled distance is concerned. Figure 3 indicates the maximum deflection

excluding the RBM decreases with the increase of the scaled distance, so do the maximum gross velocity and acceleration. It is desirable to know the upper and lower bounds of maximum acceleration are close to each other. One can read the approximate peak acceleration of the structural element for specific scaled distance readily.

Recall that in deriving the RBM response, the friction between the side walls and surrounding soil and some resistances from the back side are neglected. From the results above, the ignored items are not significant compared to the considered ones. The reason is if the effects of the ignored items are significant and incorporated into the calculation, the lower bound response will become remarkably higher, much closer to the upper bound. However, the upper and lower bounds are sufficiently close to each other and there is not much room for the lower bound to become higher (for instance, of most significance, consider the gross acceleration of the structural element).

To validate the method used in the present study, the structural dimension along the direction parallel to the blast load is increased to a large value thus the mass of the structure is large. Figure 4 indicates that the lowered bounds of the responses including maximum deflection, maximum gross velocity and maximum gross acceleration are very close to, and even coincide with the upper bound responses respectively, confirming the methodology to calculate the lower bound of the gross responses of the structural element.

Further, the influence of different surrounding soils on the gross responses of the

structural element is investigated. The average values of the response bounds, rather than the bounds themselves, are calculated and plotted against scaled distance. Figure 5 indicates that the maximum displacement excluding the RBM decreases with the increase of the scaled distance, so do the maximum gross velocity and acceleration. Among the response quantities, the most significant one is the maximum acceleration. Different from the maximum displacement exclusive of the RBM and maximum gross velocity, the maximum gross acceleration is highly sensitive to soil types. For instance, for the same structure and the same scaled distance, the maximum gross acceleration may be 10 times greater when buried in the Bukit Timah soil than in dry sand. Therefore, it can be stated that for safety purpose, a buried structure should be installed in a site with small acoustic impedance and large attenuation factor such as the dry sand.

In TM-5-855-1, the maximum acceleration prediction of a buried structure under a subsurface blast load is rather coarse since only an average acceleration value across the structure in a RBM manner is given, in which the density of the surrounding soil and more importantly, the information of the structure is missing, such as the material density, the thickness of the structure element and how hollow the structure is. In the perspective of the shock mechanism, the model in the present study is more reasonable, where both the effects from the RBM and the local deflection are considered. Therefore, this model may be used as a supplement to the design codes.

Response spectrum analysis of in-structure shock

Underground structure subjected to subsurface detonation undergoes rigid body motion as a whole and local deflection of its structural elements, posing a shock excitation for the equipments and personnel within the structure. Devices, with their fixtures combined together can be simplified as SDOF systems, shown in Fig. 6. The mass and stiffness of an SDOF system can be represented by only one parameter: the natural frequency. Then a series of SDOF systems of varying natural frequencies can represent a variety of devices with supports. When the shock input does not exceed the equipment tolerance, the equipment can be hard-mounted to the structure. For instance, if a device is small and rugged, it is usually hard-mounted as it could withstand high accelerations. However, those devices that cannot withstand such strong shock should be shock-isolated.

Shock response spectra are a series of relationships between the maximum responses of SDOF systems and their corresponding natural frequencies under the same base excitation (Gupta 1990). For each SDOF system, the absolute maximum value of the response of interest from the corresponding time history is calculated. In response calculation, the sign is often not considered since, for design purpose, the maximum positive and negative values are assumed to have equal effect.

In the present study, it is assumed that the mass of the structural element is significantly larger than that of the device with mounting thus the responses of the device and the structural element can be decoupled. When analyzing the responses of the structural element, the effect from the attached device is ignored. Then the gross acceleration time history of the structural element center is used to excite the attached

devices.

Figure 7 is the total shock response spectra for the current case study. Generally, systems with lower natural frequencies undergo higher displacements, while the systems with higher natural frequencies experience higher accelerations instead. For a series of SDOF systems with different natural frequencies, those with mediate natural frequencies have larger velocity responses.

Table 2 lists some typical equipment shock tolerances (U.S. Army 1986). For a specific underground detonation, the shock level to the equipment can be readily obtained using the present method. Comparison of these shock values, especially the maximum accelerations, with their corresponding tolerances (drawn in Fig. 7) indicates whether the equipment is safe under such shock. If the shock tolerance is exceeded, isolation is needed. For the specific shock parameters applied in this study, the response spectra are plotted against the equipment natural frequencies. From Fig. 7, for a specific device, the stiffness of the system consisting of the device and its fixture should not exceed a certain value.

In simple summary, an integrated analytical prediction method is proposed to evaluate the shock level within an underground structure subjected to a subsurface explosion. This method can also be extended to evaluate the shock level within a submarine subjected to an underwater explosion, shock of nuclear power plant and shock caused by launching and landing of spacecrafts, etc., since these shocks and vibrations may have the similar nature to the one induced by a subsurface detonation.

Conclusions

In-structure shock evaluation of an underground structures subjected to a subsurface detonation, especially the structural shock response, is investigated analytically. An interfacial damping is incorporated to represent the soil-structure interaction. Rigid body motion of the structure as a whole and the local structural element deflection are analyzed. Shock response spectra are employed to evaluate the shock level within the structure. Comparison of the equipment shock level with the shock tolerance indicates whether the built-in equipment or device is safe or shock isolation is needed. The maximum deformation, gross velocity and gross acceleration are greater in soil with larger acoustic impedance and smaller attenuation factor, which results in higher equipment shock level and, thus, more detrimental. Especially, the maximum acceleration of the structural element is highly sensitive to soil types, thus the protective structure is better constructed in a site with small acoustic impedance and large attenuation factor for safety purpose. Results show that the proposed in-structure shock assessment method is effective and can be used as a supplement to TM-5-855-1 and TM-5-1300.

Notation

The following symbols are used in this paper:

A area of the structural element closest to the subsurface detonation;

a, b in-plane dimension;

c_s acoustic velocity of the surrounding soil;

D flexural rigidity of the structural element;

E	Young's modulus of the structure material;
f	coupling factor of the explosion energy to soil;
h	thickness of the structural element;
h_e	effective thickness of the whole structure;
M	mass of the whole structure;
P_0	free-field peak pressure;
R	distance from center of explosion to structure;
r	attenuation coefficient of blast wave in soil;
T_d	blast duration;
t	time starting at the arrival of the blast wave;
t_a	travel time of shock wave from detonation to structure;
$U(t)$	rigid body motion displacement of the whole structure;
W	TNT equivalent charge weight;
$w(x,y,t)$	gross displacement time history of the structural element;
$W_{mn}(x,y)$	*m*, *n*th mode shape of the structure element;
$w_{mn}(x,y,t)$	*m*, *n*th mode contribution to pure deflection of the structural element;
x, y	in-plane coordinate with origin at a corner;
α	reduction factor;
β	a factor equal to 160 in imperial unit system;
$\eta_{mn}(t)$	*m*,*n*th mode general coordinate;
σ_f	free-field pressure time history;
ρ, ρ_s	mass density of the structure and soil;

ζ_{mn} *m*, *n*th mode interfacial damping ratio;

ν Poisson's ratio of the structural material;

τ_0 characteristic response time of the whole structure;

ω_{mn} *m*, *n*th mode natural frequency of the structural element.

Subscripts

m mode order in direction along edge *a*;

n mode order in direction along edge *b*.

References

Alwis, W. A. M., Lam, K. Y. (1994). "Response spectrum of underground protective structures." *Finite Elem. Anal. Des.*, 18, 203–209.

Anand S. (2007). "Measurement and modeling of ground response due to dynamic loading." Ph.D. thesis, Nanyang Technological Univ., Singapore.

Baylot, J. T., Hall, R. L. (1995). "Effect of rigid-body motion on small-scale soil-structure interaction experiments." *Proc., Pressure Vessels and Piping Conf.*, joint ASME/ASCE, Honolulu, Hawaii, 47–56.

Baylot, J. T. (2000). "Effect of soil flow changes on structure loads." *J. Struct. Eng.*, 126(12), 1434–1441.

Chen, H. L., Chen, S. E. (1996). "Dynamic response of shallow-buried flexible plates subjected to impact loading." *J. Struct. Eng.*, 122(1), 55–60.

Chen, Y., Krauthammer, T. (1989). "A combined Adina-finite difference approach with substructure for solving seismically induced nonlinear soil-structure

interaction problems." *Comp. Struct.*, 32(3–4), 779–785.

Gupta, A. K. (1990). *Response spectra method in seismic analysis and design of structures*, Blackwell scientific publications, Boston.

Lu, Y., Wang, Z. Q. and Chong, K. (2005). "A comparative study of buried structure in soil subjected to blast load using 2D and 3D numerical simulation." *Soil Dyn. Earthq. Eng.*, 25, 275–288.

Stamos, A. A., Beskos, D. E. (1992). "Dynamic analysis of large 3-D underground structure by the BEM." *Earthq. Eng. Struct. Dyn.*, 24, 917–934.

Stevens, D. J., Krauthammer, T. (1988). "A finite difference/finite element approach to dynamic soil-structure interaction modeling." *Comp. Struct.*, 29(2), 199–205.

U.S. Army. (1986). "Fundamentals of protective design for conventional weapons." TM-5-855-1, U.S. Army, Washington, D.C.

U.S. Army. (1990). "Structures to resist the effects of accidental explosions." TM-5-1300, U.S. Army, Washington, D.C.

Wang, Z. Q., Lu, Y., Hao, H. and Chong, K. (2005). "A full coupled numerical analysis approach for buried structures subjected to subsurface blast." *Comp. Struct.*, 83, 339–356.

Weidlinger, P., Hinman, E. (1988). "Analysis of underground protective structures." *J. Struct. Eng.*, 114(7), 1658–1673.

Weidlinger, P., Hinman, E. (1991). "Cavitation in solid medium." *J. Eng. Mech.*, 117(1), 166–183.

Wong, F. S., Weidlinger, P. (1983). "Design of underground protective structures." *J.*

Struct. Eng., 109(8), 1972–1979.

Wong, F. S (1984). "Uncertainties in dynamic soil-structure interaction." *J. Eng. Mech.*, 110(2), 308–324.

Yang, W. (1997). "Finite element simulation of response of buried shelters to blast loadings." *Finite Elem. Anal. Des.*, 24, 113–132.

Figure captions

Fig. 1. Underground structure subjected to subsurface detonations

Fig. 2. Time histories of upper and lower bounds of deformation, gross velocity and gross acceleration at the structural element center, Kallang soil

(a) Deformation

(b) Gross velocity

(c) Gross acceleration

Fig. 3. Upper and lower bounds of maximum deformation, gross velocity and gross acceleration at the structural element center versus scaled distance, Kallang soil

(a) Maximum deformation

(b) Maximum gross velocity

(c) Maximum gross acceleration

Fig. 4. Upper and lower bounds of maximum deformation, gross velocity and gross acceleration at the structural element center versus scaled distance, Kallang soil (dimension in movement direction = 300 m, for validation of the solution)

(a) Maximum deformation

(b) Maximum gross velocity

(c) Maximum gross acceleration

Fig. 5. Maximum deformation, gross velocity and gross acceleration of structural element center versus scaled distance, different soils:

(a) Maximum deformation

(b) Maximum gross velocity

(c) Maximum gross acceleration

Fig. 6. Illustration of SDOF systems for shock response spectra

Fig. 7. Shock response spectra of devices subjected to in-structure shock, Kallang soil

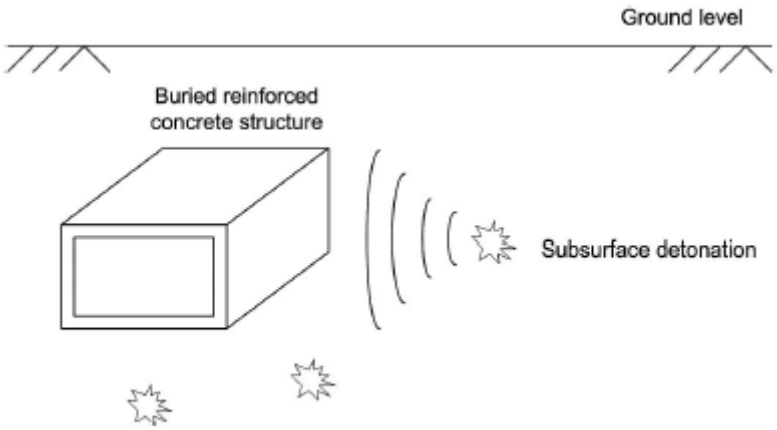

Fig. 1. Underground structure subjected to subsurface detonations

Fig. 1

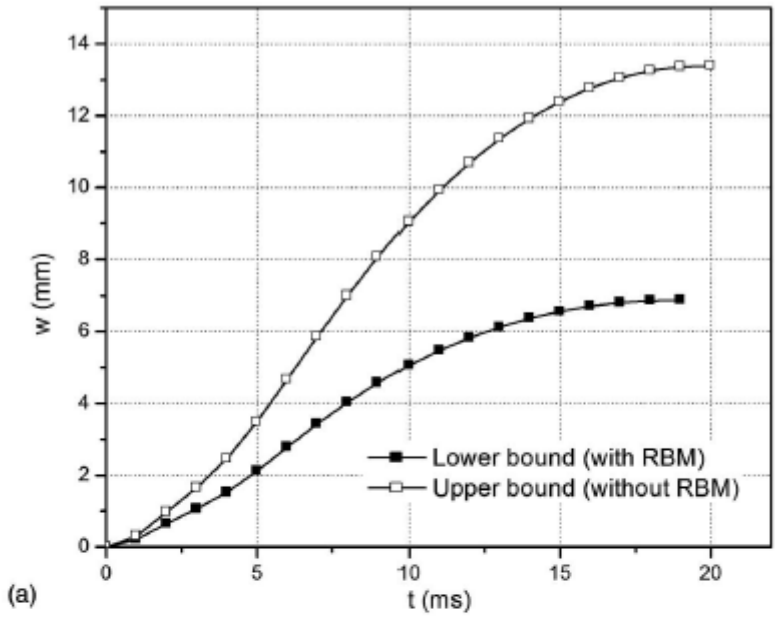
w (mm)
t (ms)
Lower bound (with RBM)
Upper bound (without RBM)

(a)

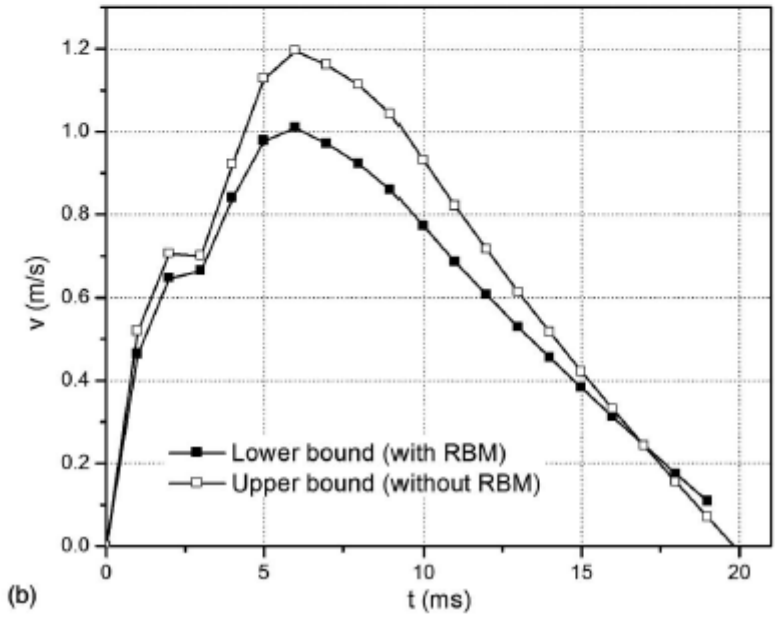
v (m/s)
t (ms)
Lower bound (with RBM)
Upper bound (without RBM)

(b)

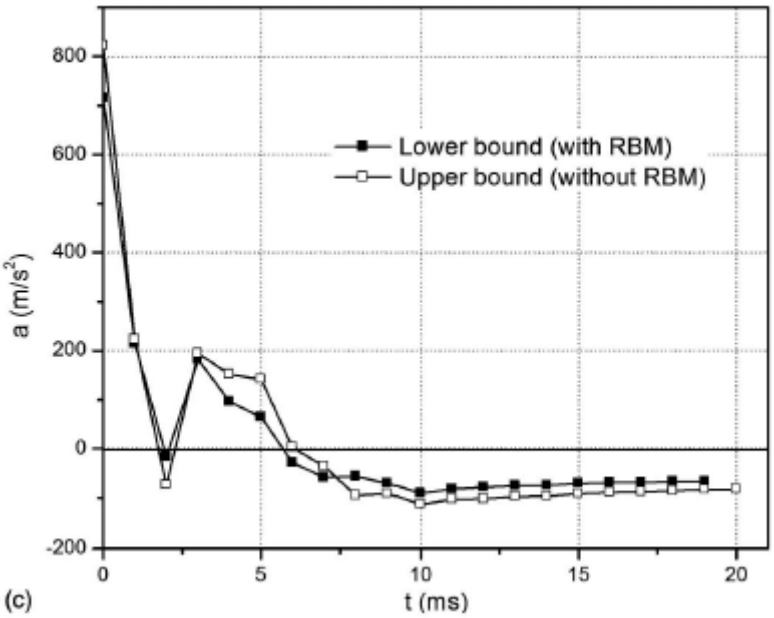
800
600
400
200
0
-200
a (m/s^2)
0
5
10
15
20
t (ms)
Lower bound (with RBM)
Upper bound (without RBM)
(c)

Fig. 2

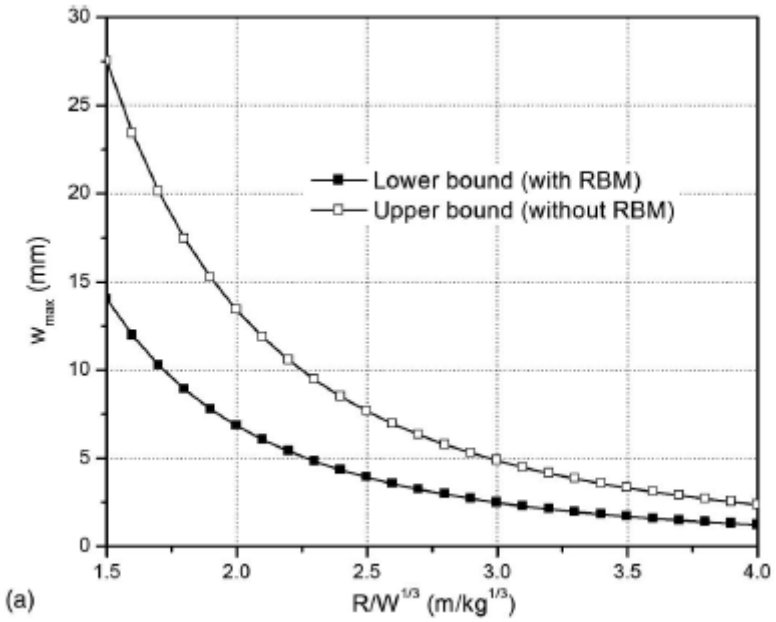
Lower bound (with RBM)
Upper bound (without RBM)
w_{max} (mm)
$R/W^{1/3}$ (m/kg$^{1/3}$)
(a)

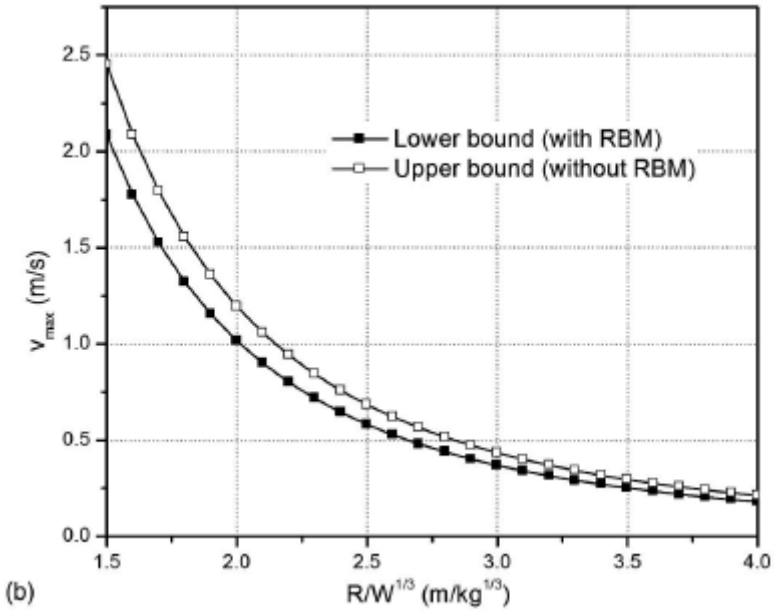
Lower bound (with RBM)
Upper bound (without RBM)
v_{max} (m/s)
$R/W^{1/3}$ (m/kg$^{1/3}$)
(b)

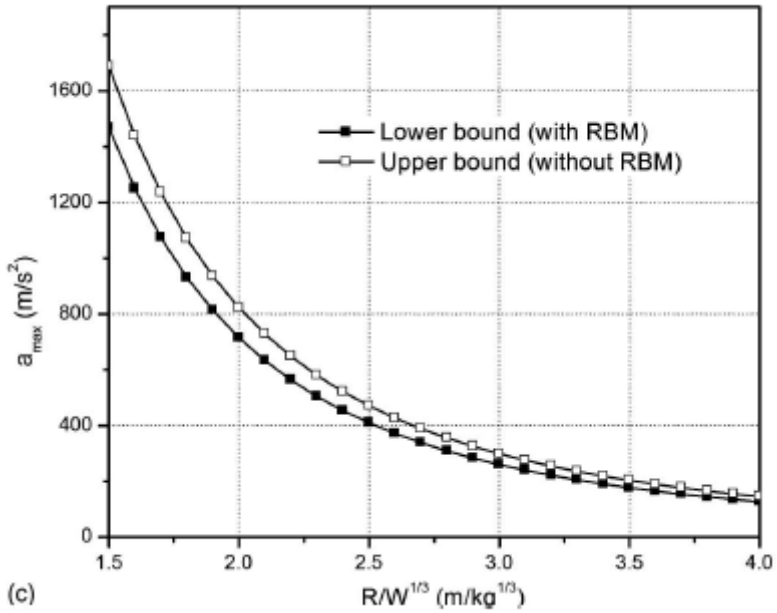
Lower bound (with RBM)
Upper bound (without RBM)
1600
1200
800
400
0
1.5
2.0
2.5
3.0
3.5
4.0
a_{max} (m/s^2)
R/W$^{1/3}$ (m/kg$^{1/3}$)
(c)

Fig. 3

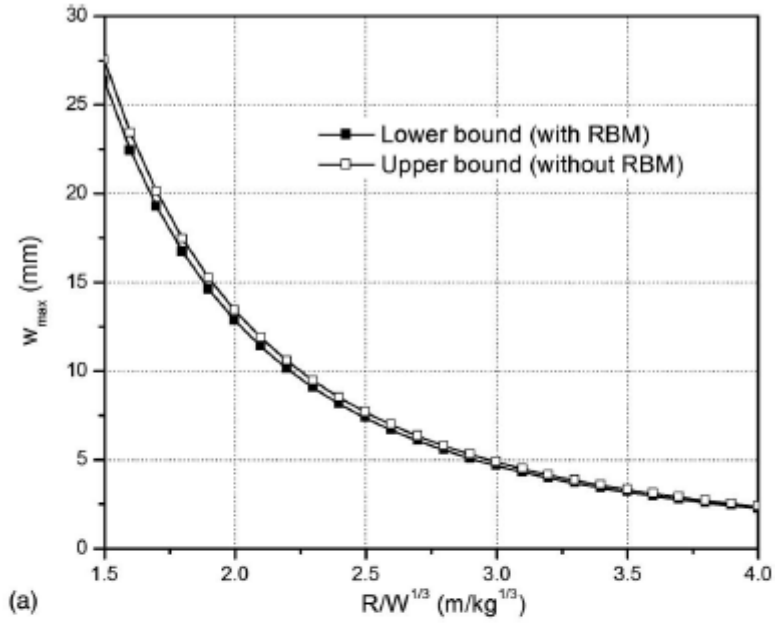
Lower bound (with RBM)
Upper bound (without RBM)
w_{max} (mm)
$R/W^{1/3}$ (m/kg$^{1/3}$)
(a)

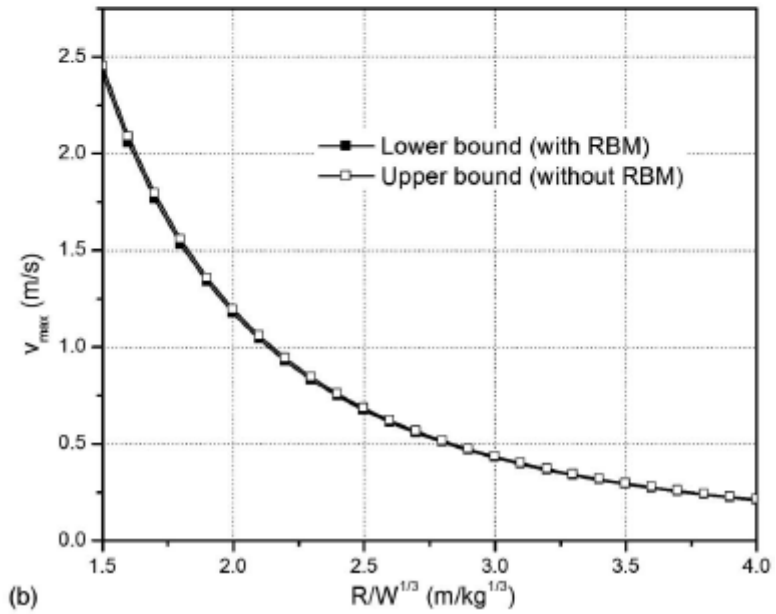
Lower bound (with RBM)
Upper bound (without RBM)
v_{max} (m/s)
$R/W^{1/3}$ (m/kg$^{1/3}$)
(b)

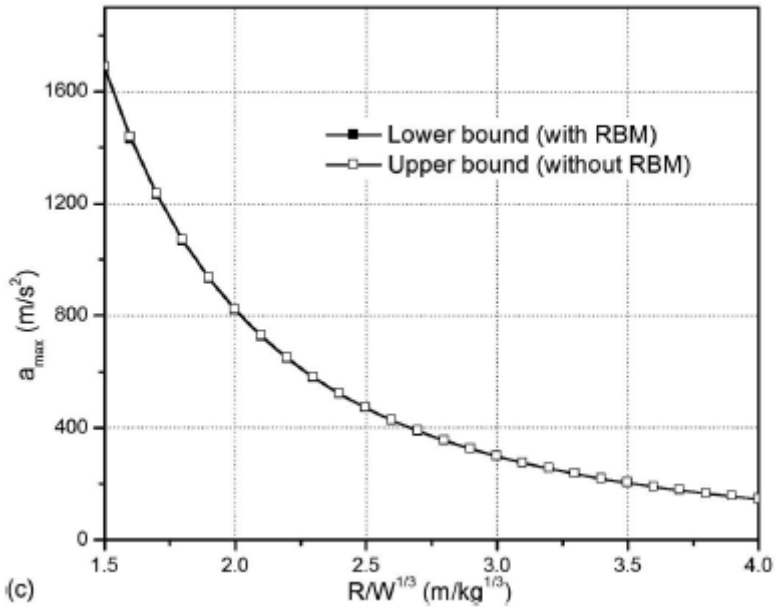
Lower bound (with RBM)
Upper bound (without RBM)
1600
1200
800
400
0
1.5
2.0
2.5
3.0
3.5
4.0
a_{max} (m/s^2)
R/W$^{1/3}$ (m/kg$^{1/3}$)
(c)

Fig. 4

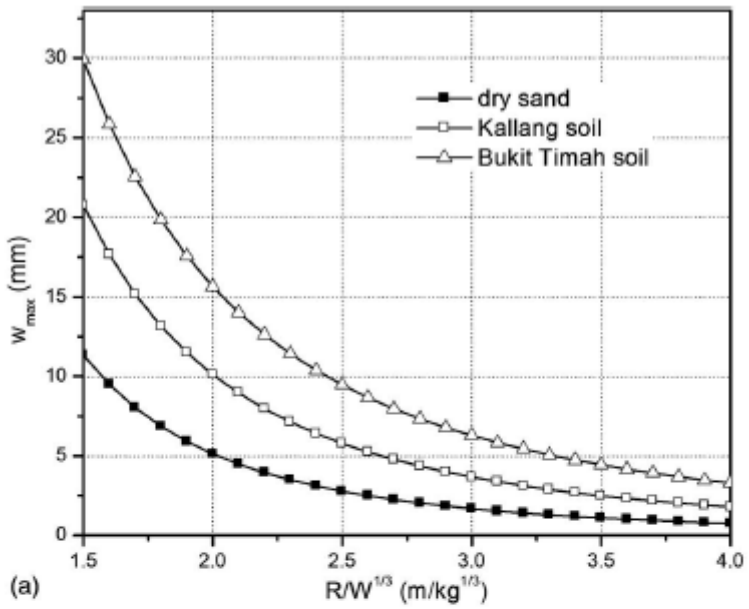
dry sand
Kallang soil
Bukit Timah soil
w_{max} (mm)
$R/W^{1/3}$ (m/kg$^{1/3}$)
(a)

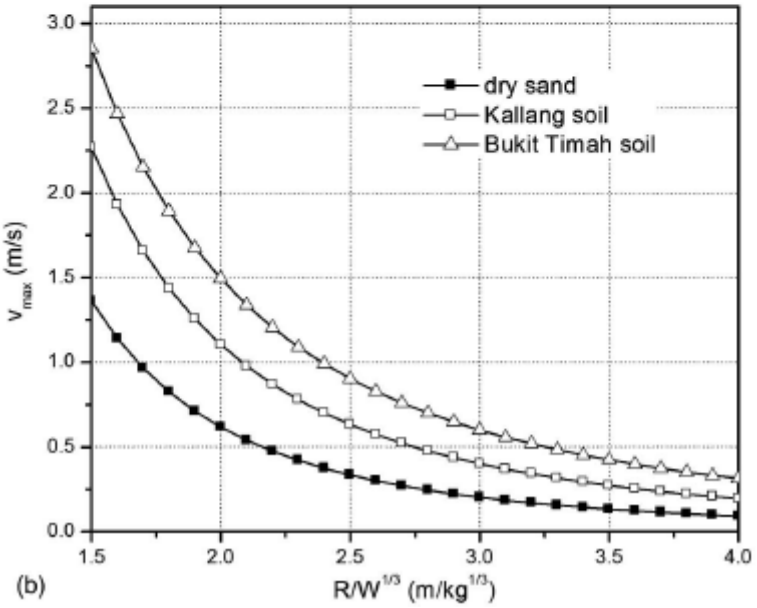
dry sand
Kallang soil
Bukit Timah soil
v_{max} (m/s)
$R/W^{1/3}$ (m/kg$^{1/3}$)
(b)

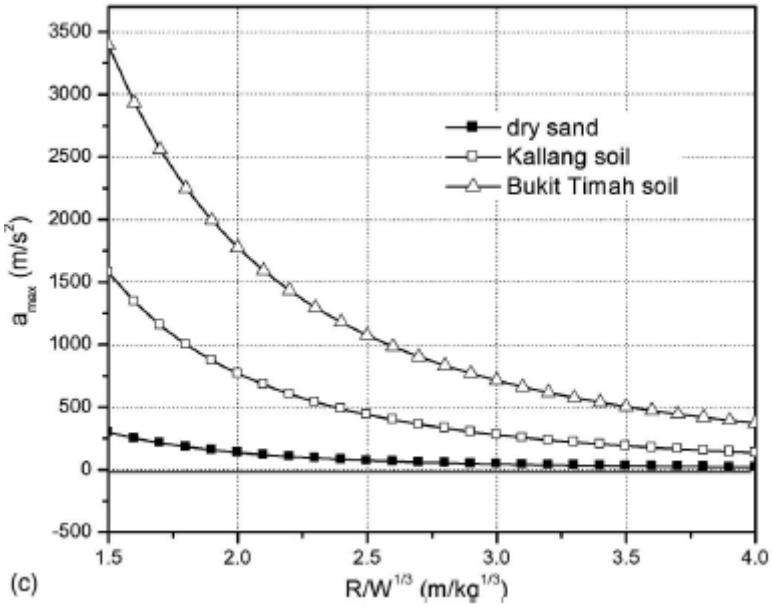
3500
3000
2500
2000
1500
1000
500
0
-500
1.5
2.0
2.5
3.0
3.5
4.0
dry sand
Kallang soil
Bukit Timah soil
a_{max} (m/s^2)
R/W$^{1/3}$ (m/kg$^{1/3}$)
(c)

Fig. 5

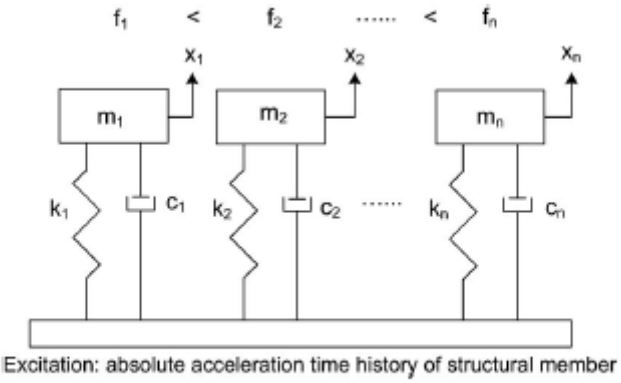

Fig. 6. Illustration of SDOF systems for shock response spectra

Fig. 6

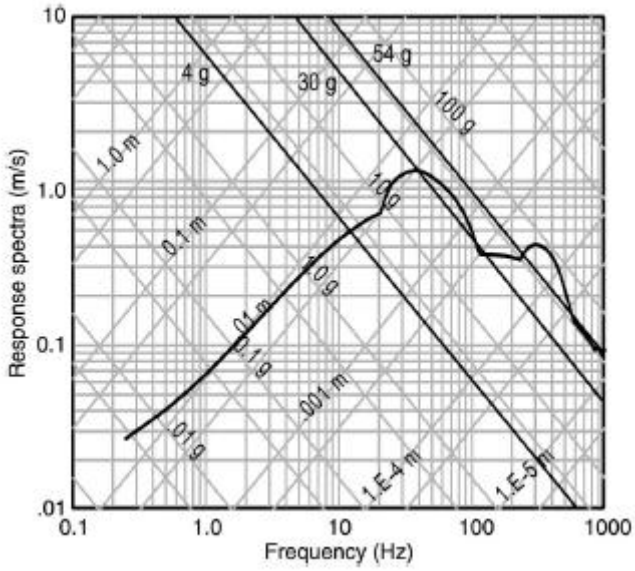
Response spectra (m/s)
Frequency (Hz)
10
1.0
0.1
.01
0.1
1.0
10
100
1000
4 g
30 g
54 g
100 g
1.0 m
0.1 m
.01 m
.001 m
1E-4 m
1E-5 m
1.0 g
0.1 g
.01 g

Fig. 7

Table 1 Properties of dry sand and two typical soils in Singapore.

Soil type	Density (kg/m^3)	Acoustic velocity (m/s)	Attenuation coefficient
Dry sand	1633	305	2.75
Kallang soil	1420	1350	2.5
Bukit Timah soil	1800	1650	2.25

Table 2 Equipment shock resistance

Item	Horizontal tolerance (g's)	Vertical tolerance (g's)
Air handling units	4	4
Diesel engine generators	30	30
Gas turbine generators	31	4
Computers	53	54